Supplemental Information for

Role of the Hydrophobic Bridge in the Carbapenemase Activity of Class D β-Lactamases

Nichole K. Stewart[a], Clyde A. Smith[b], Nuno T. Antunes[a], Marta Toth[a], Sergei B. Vakulenko[a]

[a]Department of Chemistry and Biochemistry, University of Notre Dame, Notre Dame, Indiana, USA

[b]Stanford Synchrotron Radiation Lightsource, Stanford University, Menlo Park, California, USA

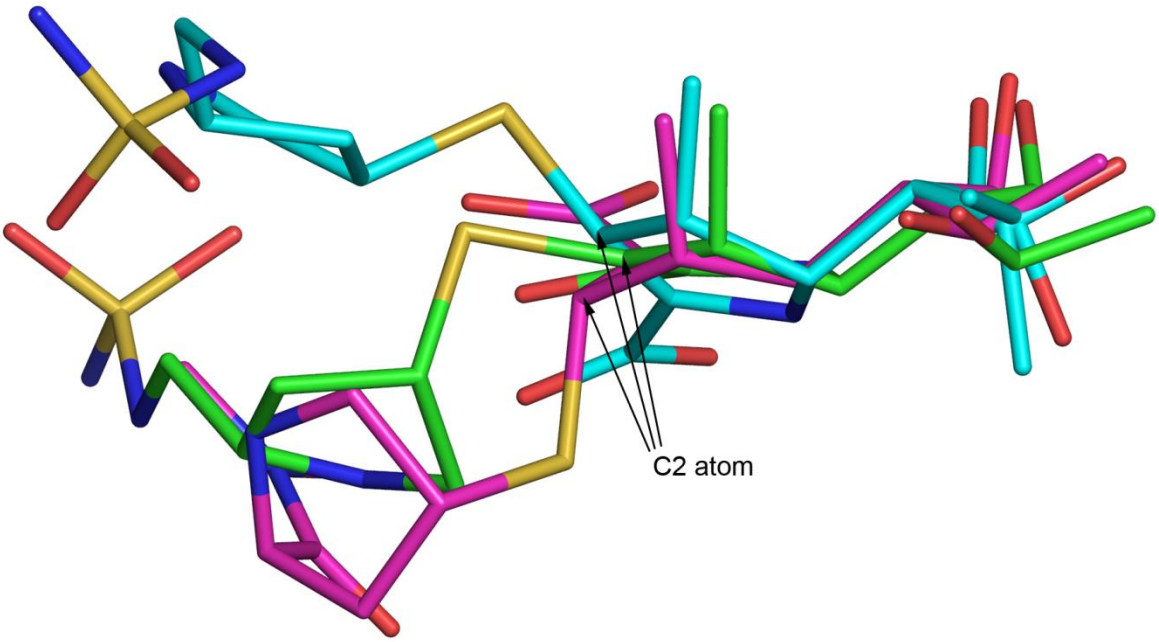

FIGURE S1. Comparison of the three possible tautomers for a carbapenem. The Δ^2 tautomer is derived from the structure of doripenem-OXA-24 (green sticks; PDB code 3PAE). The Δ^1R isomer is derived from the doripenem-OXA-1 structure (cyan; PDB code 3ISG). The Δ^1S isomer is derived from the meropenem-OXA-23 structure (magenta; PDB code 4JF4). The C2 atom is indicated for all three tautomers.

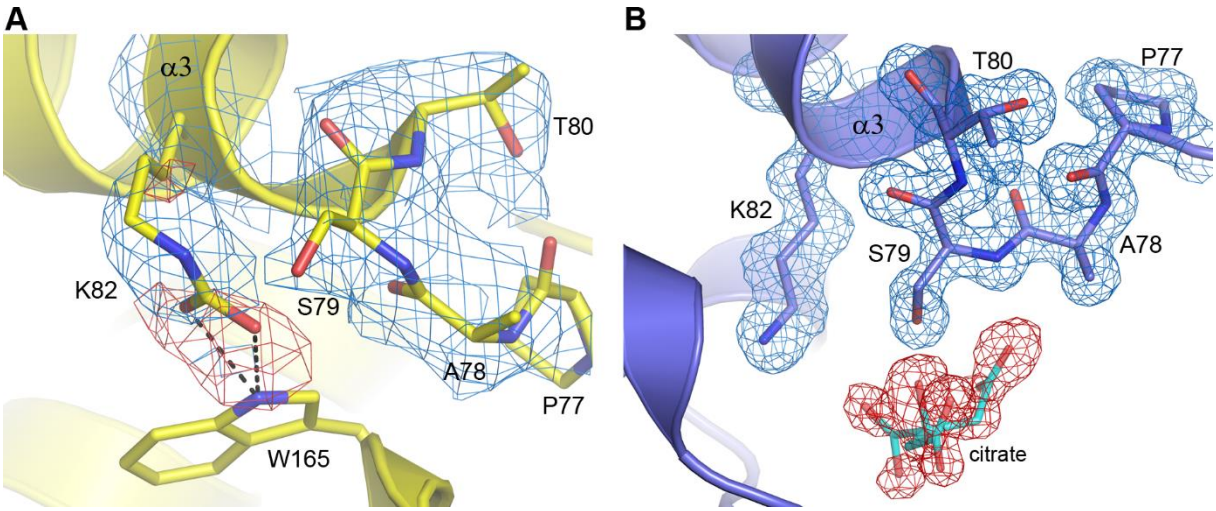

FIGURE S2. Electron density for the F110A/M221A OXA-23 mutant structures. (A) Final $2F_o$-F_c density (blue mesh, 1.0 σ) in the active site of the neutral pH apo structure. The catalytic residues (Ser79 and Lys82) are shown, along with residues neighboring the serine (Ala78 and Thr80). Residual F_o-F_c density calculated following molecular replacement is shown as a red mesh (contoured at 2.75 σ), indicating the presence of a carboxylate moiety on Lys82. The carboxylate group was omitted from the molecular replacement calculation, and the carboxylated Lys82 is shown here in its final refined position. The side chain of Trp165 from the Ω-loop is involved in the stabilization of the carboxylated Lys82 via hydrogen bonding interactions (black dashed lines). (B) Final $2F_o$-F_c density (blue mesh, 1.0 σ) in the active site of the low pH apo structure. The catalytic residues (Ser79 and Lys82) are shown, along with residues neighboring the serine (Pro77, Ala78 and Thr80). No residual F_o-F_c density is observed at the end of the Lys82 side chain, indicating that the lysine residue is not modified by carboxylation. A large piece of residual F_o-F_c density near the catalytic serine was modeled as citrate (shown as semi-transparent cyan sticks from the final refined structure).

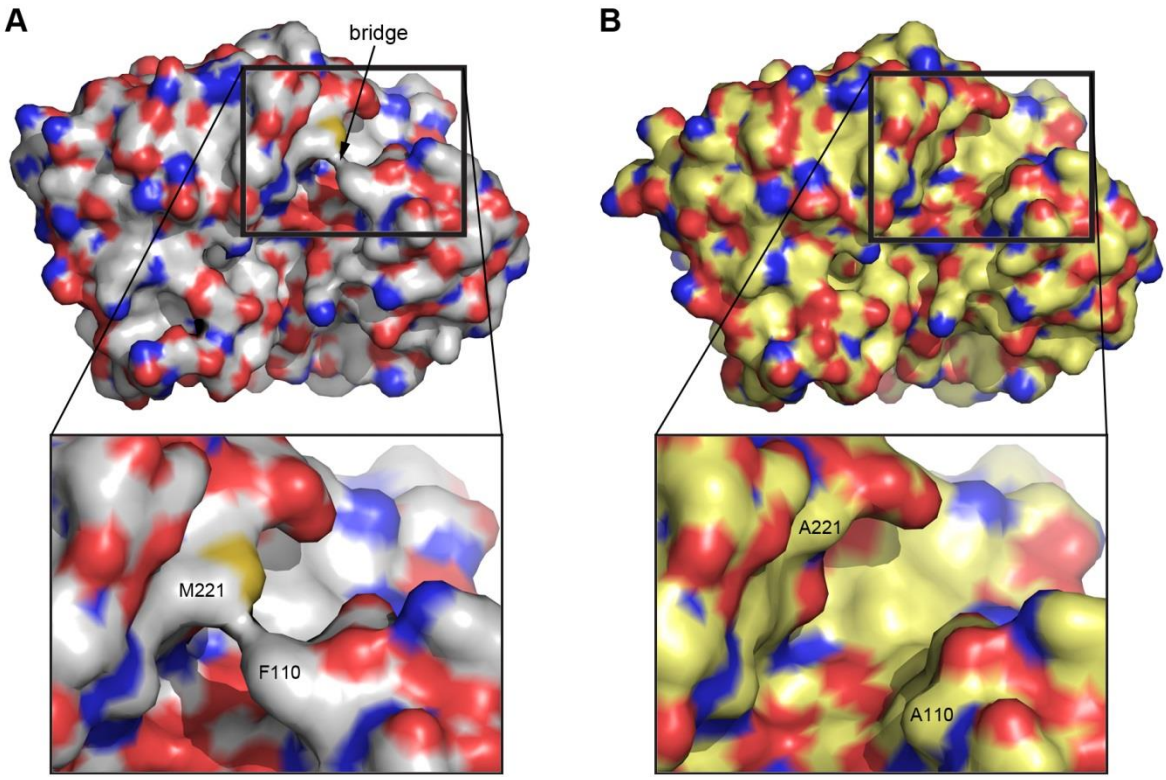

FIGURE S3. Molecular surface representation of wild-type and mutant OXA-23. (A) Molecular surface representation of wild-type OXA-23 showing the location of the hydrophobic bridge across the active site. The close up (lower panel) shows the location of Phe110 and Met221 of the bridge. (B) Molecular surface representation of the F110A/M221A OXA-23 mutant. The close up (lower panel) shows the location of Ala110 and Ala221.

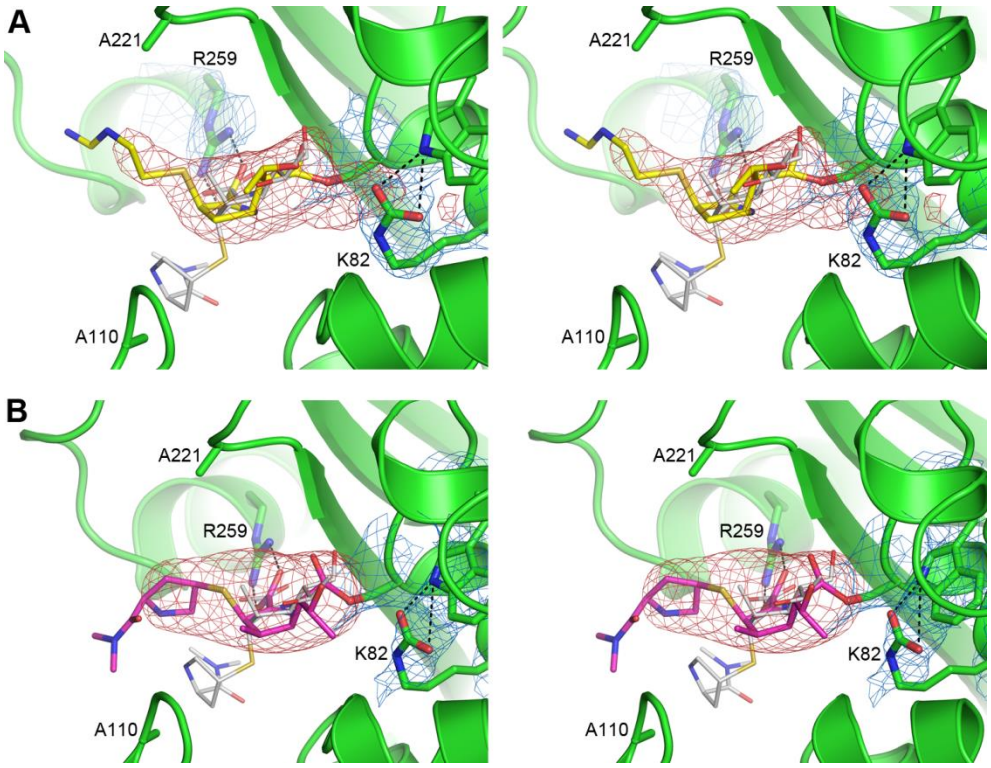

FIGURE S4. Stereoviews of the electron density for the F110A/M221A OXA-23 neutral pH complexes. (A) Two minute soak with imipenem, showing the residual F_o-F_c density (pink mesh, 4.0 σ) following molecular replacement. The refined F110A/M221A OXA-23 structure is shown as green cartoon and green sticks for the side chains of the catalytic residues (Ser79 and Lys82), the two mutated residues (Ala110 and Ala221), the arginine (Arg259) which interacts with the carboxylate of the bound substrate, and Trp165 (left side of the panel, no label) which hydrogen bonds to the carboxylated Lys82. Final 2F_o-F_c density calculated is shown as a blue mesh (contoured at 1.2 σ) for Ser79, Lys82 and Arg259. The imipenem acyl-enzyme intermediate from the final refined model at 3.1 Å resolution is shown in yellow in a Δ^1R configuration. The Δ^1S tautomer of meropenem bound to wild-type OXA-23 (PDB code 4JF4) is shown as thin gray sticks for comparison. (B) Two minute soak with meropenem, showing the residual F_o-F_c density (pink mesh, 4.3 σ) following molecular replacement. The refined F110A/M221A OXA-23 structure is shown as green cartoon and green sticks for the side chains of Ser79, Lys82, Ala110, Ala221, Arg259 and Trp165 (no label). Final 2F_o-F_c density calculated is shown as a blue mesh (contoured at 1.0 σ) for Ser79 and Lys82. The meropenem acyl-enzyme intermediate from the final refined model at 3.5 Å resolution is shown in magenta in a Δ^1R configuration, and represents the best fit (compared to Δ^1S and Δ^2 tautomers) to this residual density. The Δ^1S tautomer of meropenem bound to wild-type OXA-23 (PDB code 4JF4) is shown as thin gray sticks for comparison.

Table S1. Tautomeric conformations of class D β-lactamases

Enzyme	Source	Mutation	Phe-Met Bridge	Carbapenem	Tautomer	PDB code	Reference
OXA-1	*E. coli*	WT	No	doripenem	Δ^1R	3ISG	(1)
OXA-13	*P. aeruginosa*	WT	No[a]	imipenem	Δ^2	1H5X	not publ.
OXA-13	*P. aeruginosa*	WT	No[a]	meropenem	Δ^2	1H8Y	(2)
OXA-23	*A. baumannii*	WT	Yes	meropenem	Δ^1S	4JF4	(3)
OXA-24/40	*A. baumannii*	V130D	Yes	doripenem	Δ^2	3PAG	(4)
OXA-24/40	*A. baumannii*	K84D	Yes	doripenem	Δ^2	3PAE	(4)
OXA-51	*A. baumannii*	I129L/K83D	Yes[b]	doripenem	Δ^2	5L2F	(5)
OXA-239	*A. baumannii*	K82D	Yes	doripenem	Δ^2	5WI7	(6)
OXA-239	*A. baumannii*	K82D	Yes	imipenem	Δ^1R[c]	5WIB	(6)
OXA-23	*A. baumannii*	F110A/M221A	No	imipenem	Δ^1R		this work
OXA-23	*A. baumannii*	F110A/M221A	No	meropenem	Δ^1R		this work
OXA-23	*A. baumannii*	F110A/M221A	No	imipenem	Δ^1R		this work
OXA-23	*A. baumannii*	F110A/M221A	No	meropenem	Δ^1R		this work
BPU-1	*B. pumilus*	WT	No	doripenem	Δ^1R	5CTN	(7)

[a] Structure and sequence differences in the loop preceding the C-terminal helix alters the orientation of the Phe208 side chain which now occupies the Met221 position.
[b] The bridge residues are Phe111 and Trp222. The Trp222 side chain rotates by 180° to accommodate the doripenem (8).
[c] The imipenem has no tail (truncated at the sulfur).

Table S2. Low pH form data collection statistics

OXA-23 mutant low pH form			
	apo	**meropenem**	**imipenem**
Space group	$P2_12_12$	$P2_12_12$	$P2_12_12$
Unit cell, *a,b,c* (Å)	136.58, 43.99, 46.55	136.12, 44.01, 46.22	136.16, 44.20, 46.63
Resolution (Å)	38.5-1.25 (1.27-1.25)[a]	38.2-1.55 (1.58-1.55)	38.5-1.55 (1.58-1.55)
Reflections			
- observed/unique	996824 / 77596	297149 / 41163	294728 / 41640
R_{meas}[b]	6.7 (89.1)	7.2 (107.8)	6.2 (94.7)
R_{pim}[b]	1.9 (24.6)	2.6 (41.4)	2.3 (35.9)
$I / \sigma I$	14.7 (1.4)	12.8 (1.6)	17.4 (1.9)
Completeness (%)	99.9 (94.7)	99.8 (97.8)	99.6 (97.8)
CC½[c]	0.999 (0.887)	0.998 (0.777)	0.999 (0.862)
Average multiplicity	12.8 (12.3)	7.2 (6.4)	7.1 (6.7)
Wilson B ($Å^2$)	14.3	21.4	19.2

[a] Numbers in parentheses refer to the highest resolution shell.
[b] R_{meas} is the redundancy-independent merging R factor, and R_{pim} is the precision-indicating merging R factor (9).
[c] Correlation between intensities from random half-sets of data (10).

Table S3. Neutral pH form data collection statistics

OXA-23 mutant neutral pH form			
	apo	**meropenem**	**imipenem**
Space group	I422	I422	I422
Unit cell, *a,c* (Å)	175.18, 79.22	175.24, 81.18	174.88, 81.30
Resolution (Å)	39.2-3.25 (3.51-3.25)[a]	39.2-3.5 (3.83-3.5)	39.1-3.10 (3.31-3.10)
Reflections			
- observed/unique	93160 / 9985	117920 / 8247	171217 / 11718
R_{meas}[b]	16.9 (92.1)	26.2 (207.1)	18.9 (115.2)
R_{pim}[b]	5.7 (30.4)	5.9 (54.9)	4.9 (29.1)
$I / \sigma I$	9.8 (2.4)	9.4 (1.5)	10.8 (2.3)
Completeness (%)	99.8 (99.7)	99.9 (99.9)	99.9 (99.7)
CC½[c]	0.997 (0.885)	0.993 (0.900)	0.995 (0.904)
Average multiplicity	9,3 (8.9)	14.3 (13.9)	7.8 (8.0)
Wilson B ($Å^2$)	79.9	83.5	86.9

[a] Numbers in parentheses refer to the highest resolution shell.
[b] R_{meas} is the redundancy-independent merging R factor, and R_{pim} is the precision-indicating merging R factor (9).
[c] Correlation between intensities from random half-sets of data (10).

Table S4. Low pH structure refinement statistics

	OXA-23 mutant low pH form		
	apo	**meropenem**	**imipenem**
pH	4.1	4.6	4.6
Resolution (Å)	38.47 – 1.25	37.0 – 1.55	37.1 – 1.55
Reflections used, work / free	73880 / 3762	39038 / 2093	39486 / 2126
R_{work} / R_{free} [a]	0.1543 / 0.1799	0.1722 / 0.1917	0.1767 / 0.1962
Number of atoms			
- protein	1881	1819	1890
- ligand/ions	13 (citrate)	26 (meropenem)	20 (imipenem)
- water	262	168	210
B-factors (Å^2)			
- protein	21.4	25.0	23.2
- ligand	24.1	35.6	30.0
- water	36.0	37.1	35.6
rms deviations			
- bond lengths (Å)	0.005	0.006	0.006
- bond angles (°)	1.15	0.975	0.916
Ramachandran plot[b]			
- residues in favored regions (%)	98.2	97.3	96.7
- number of outliers	1	1	0
Molprobity score[b]	1.13	1.24	1.70

[a] R_{free} was calculated using a test set comprising 5% of the data.
[b] Calculated with the program MOLPROBITY (11).

Table S5. Neutral pH structure refinement statistics

	OXA-23 mutant neutral pH form		
	apo	**meropenem**	**imipenem**
Resolution (Å)	39.2 – 3.25	39.2 – 3.50	39.1 – 3.10
Reflections used, work / free	9480 / 484	7147 / 385	11708 / 570
R_{work} / R_{free} [a]	0.2450 / 0.2903	0.2339 / 0.2998	0.1902 / 0.2162
Number of atoms			
- protein	1899	1896	1908
- ligand/ions	-	26 (meropenem)	25 (imipenem)
B-factors (Å^2)			
- protein	94.2	130.8	95.1
- ligand	-	136.9	103.3cd ../
rms deviations			
- bond lengths (Å)	0.010	0.003	0.009
- bond angles (°)	1.10	0.700	1.10
Ramachandran plot[b]			
- residues in favored regions (%)	89.4	95.7	93.2
- number of outliers	3	0	1
Molprobity score[b]	3.27	1.95	2.39

[a] R_{free} was calculated using a test set comprising 5% of the data.
[b] Calculated with the program MOLPROBITY (11).

References

1 Schneider KD, Karpen ME, Bonomo RA, Leonard DA, Powers RA. 2009. The 1.4 Å crystal structure of the class D β-lactamase OXA-1 complexed with doripenem. Biochemistry 48:11840-11847.

2. Pernot L, Frénois F, Rybkine T, L'Hermite G, Petrella S, Delettré J, Jarlier V, Collatz E, Sougakoff W. 2001. Crystal structures of the class D β-lactamase OXA-13 in the native form and in complex with meropenem. J Mol Biol 310:859-874.

3. Smith CA, Antunes NT, Stewart NK, Toth M, Kumarasiri M, Chang M, Mobashery S, Vakulenko SB. 2013. Structural basis for carbapenemase activity of the OXA-23 β-lactamase from *Acinetobacter baumannii*. Chem Biol 20:1107-1115.

4. Schneider KD, Ortega CJ, Renck NA, Bonomo RA, Powers RA, Leonard DA. 2011. Structures of the class D carbapenemase OXA-24 from *Acinetobacter baumanii* in complex with doripenem. J Mol Biol 406:583-594.

5. June CM, Muckenthaler TJ, Schroder EC, Klamer ZL, Wawrzak Z, Powers RA, Szarecka A, Leonard DA. 2016. The structure of a doripenem-bound OXA-51 class D β-lactamase variant with enhanced carbapenemase activity. Protein Sci 25:2152-2163.

6. Harper TM, June CM, Taracila MA, Bonomo RA, Powers RA, Leonard DA. 2018. Multiple substitutions lead to increased loop flexibility and expanded specificity in *Acinetobacter baumannii* carbapenemase OXA-239. Biochem J 475:273-288.

7. Toth M, Antunes NT, Stewart NK, Frase H, Bhattacharya M, Smith CA, Vakulenko SB. 2016. Class D β-lactamases do exist in Gram-positive bacteria. Nat Chem Biol 12:9-14.

8. Smith CA, Antunes NT, Stewart NK, Frase H, Toth M, Kantardjieff KA, Vakulenko S. 2015. Structural basis for enhancement of carbapenemase activity in the OXA-51 family of class D β‑lactamases. ACS Chem Biol 10:1791-1796.

9. Weiss MS. 2001. Glocal indicators of X-ray data quality. J Appl Crystallogr 34:130-135.

10. Karplus PA, Diederichs K. 2012. Linking crystallographic model and data quality. Science 336:1030-1033.

11. Chen VB, Arendall WB, Headd JJ, Keedy DA, Immormino RM, Kapral GJ, Murray LW, Richardson JS, Richardson DC. 2010. MolProbity: All-atom structure validation for macromolecular crystallography. Acta Crystallogr D66:12-21.